Published in final edited form as:
J Bone Miner Res. 2012 July ; 27(7): 1462–1470. doi:10.1002/jbmr.1603.

Denosumab Treatment for Fibrous Dysplasia

AM Boyce[1,2], **WH Chong**[1], **J Yao**[3], **RI Gafni**[1], **MH Kelly**[1], **CE Chamberlain**[4], **C Bassim**[5], **N Cherman**[1], **M Ellsworth**[6], **JZ Kasa-Vubu**[6], **FA Farley**[6], **AA Molinolo**[7], **N Bhattacharyya**[1], and **MT Collins**[1]

[1]Skeletal Clinical Studies Unit, Craniofacial and Skeletal Diseases Branch, National Institute of Dental and Craniofacial Research, NIH.

[2]National Institute of Child Health and Development, NIH.

[3]Radiology and Imaging Sciences, NIH.

[4]Pharmacy Department, NIH.

[5]National Institute of Dental and Craniofacial Research, NIH.

[6]University of Michigan Health Systems, Ann Arbor, MI.

[7]Oral and Pharyngeal Cancer Branch, National Institute of Dental and Craniofacial Research, NIH.

Abstract

Fibrous dysplasia (FD) is a skeletal disease caused by somatic activating mutations of the cAMP-regulating protein, $G_s\alpha$. These mutations lead to replacement of normal bone by proliferative osteogenic precursors, resulting in deformity, fracture, and pain. Medical treatment has been ineffective in altering the disease course. RANK ligand (RANKL) is a cell surface protein involved in many cellular processes, including osteoclastogenesis, and is reported to be overexpressed in FD-like bone cells. Denosumab is a humanized monoclonal antibody to RANKL approved for treatment of osteoporosis and prevention of skeletal-related events from bone metastases. We present the case of a 9-year-old boy with severe FD who was treated with denosumab for a rapidly expanding femoral lesion. Immunohistochemical staining on a pre-treatment bone biopsy specimen revealed marked RANKL expression. He was started on monthly denosumab, with an initial starting dose of 1 mg/kg and planned 0.25 mg/kg dose escalations every three months. Over seven months of treatment he showed marked reduction in pain, bone turnover markers, and tumor growth rate. Denosumab did not appear to impair healing of a femoral fracture that occurred while on treatment. With initiation of treatment he developed hypophosphatemia and secondary hyperparathyroidism, necessitating supplementation with phosphorus, calcium and calcitriol. Bone turnover markers (BTM) showed rapid and sustained suppression. With discontinuation there was rapid and dramatic rebound of BTM) with CTX (reflecting osteoclast activity) exceeding pre-treatment levels, and accompanied by severe hypercalcemia. In this child, denosumab lead to dramatic reduction of FD expansion and FD-related bone pain. Denosumab was associated with clinically significant disturbances of mineral metabolism both while on treatment and after discontinuation. Denosumab treatment of FD warrants further study to confirm efficacy and determine potential morbidity, as well as to determine the mechanism of RANKL in the pathogenesis of FD and related bone marrow stromal cell diseases.

Corresponding author: Michael T. Collins, MD Chief, Skeletal Clinical Studies Unit, CSDB, NIDCR, NIH 30 Convent Drive Building 30, Room 228, MSC 4320 Bethesda, MD 20892-4320.

DISCLOSURES

All authors state that they have no conflicts of interest.

INTRODUCTION

Fibrous dysplasia (FD, OMIM 174800) is an uncommon skeletal disorder in which normal bone and bone marrow are replaced by fibro-osseous tissue, leading to fracture, functional impairment, deformity and pain (1-3). FD may occur in association with cutaneous hyperpigmentation and hyperfunctioning endocrinopathies, including hyperthyroidism, precocious puberty, growth hormone excess, and Cushing syndrome (4-6). Skeletal lesions produce excess FGF23, leading to renal phosphate wasting, hypophosphatemia, and rickets/osteomalacia in individuals with high disease burden (7,8). FD in combination with one or more extraskeletal manifestations is termed McCune-Albright syndrome (MAS).

FD/MAS arises from activating missense mutations of the *GNAS* gene, which encodes the α-subunit of the Gs stimulatory protein ($G_s\alpha$) (9,10). Mutations occur post-zygotically resulting in a mosaic pattern of disease (11). (12). There is wide variability in both the combination of tissues involved, and the extent of involvement of affected tissue, likely arising from the fate of the specific clones that harbor the mutation at the outset (13). At the cellular level, constitutive $G_s\alpha$ activation leads to increased activity of adenylyl cyclase and excess production of intracellular cAMP. In bone, the downstream effects of constitutively elevated $G_s\alpha$ lead to an inhibition of differentiation and proliferation of bone marrow stromal cells (BMSC) (14-16). Normal bone is replaced with functionally and structurally abnormal matrix and marrow spaces show extensive fibrosis with local loss of hematopoiesis. Recently, human skeletal progenitor cells stably transfected with the FD-causing R201C $G_s\alpha$ mutation were shown to dramatically upregulate RANKL expression (17), consistent with the increased levels of osteoclastogenesis observed in FD lesions *in vivo*.

Current medical treatment for FD is palliative. Surgery is often necessary to mediate deformity and fracture, but is frequently ineffective in the setting of severe disease (18). Studies in bisphosphonates have shown consistent improvements in FD-related bone pain, but variable radiographic effects and no apparent long-term benefit on overall clinical outcomes (19-21). Additional placebo-controlled trials are needed to further define the role of bisphosphonates in treatment of FD, however at present their primary indication is limited to relief of FD-related pain.

Denosumab is a fully-humanized monoclonal antibody to RANKL recently approved for treatment of osteoporosis and skeletal-related events in adults with bone metastases from solid tumors (22,23). RANKL is expressed by osteogenic cells including osteoblasts, and plays a key role in osteoclastogenesis. By binding to its receptor on osteoclast progenitor membranes, RANKL promotes osteoclast differentiation and ultimately leads to increased bone resorption. In addition to its role in osteoclastogenesis, RANKL also plays a role in tumorigenesis in both non-skeletal (24-27) and skeletal tissues (28-30). Recent evidence suggests that the development of skeletal neoplasms depends upon activation of both RANKL and the cAMP/protein kinase A (31). RANKL inhibition via denosumab has recently been shown to be effective in treatment of giant cell granulomas of bone, which like FD are derived from BMSCs (32).

Based upon lines of evidence presented above, RANKL inhibition holds promise as a potential medical therapy for FD. We present the case of a child with FD treated with denosumab.

PATIENT AND METHODS

Clinical course

A nine-year-old boy presented with extensive polyostotic FD, hyperthyroidism, abnormalities on testicular ultrasound and café-au-lait macules, consistent with the diagnosis of MAS. The FD in his right femur underwent a dramatic expansion over an approximate four year period (Fig 1). He was treated with pamidronate for one year, which failed to slow expansion or relieve associated bone pain. Femoral expansion was associated with significant functional impairment, pain, and tachycardia from increased cardiac output. At age eight years he underwent a disarticulation amputation at the level of the femur-iliac joint. Several months later the FD in his left femur began a similar dramatic expansion, associated with significant bone pain requiring daily narcotic use. A second disarticulation amputation of his remaining lower extremity was planned. The patient's mother contacted the research team with hope that a treatment might prevent the need for amputation.

A 12-month course of denosumab was planned in an attempt to slow femoral expansion (Fig 2A). The protocol was approved by the Institutional Review Board of the NIDCR, and informed assent and consent were obtained from the patient and his mother. Denosumab was to be given once monthly, with an initial starting dose of 1 mg/kg. Dose escalations were planned at three month intervals to 1.25 mg/kg, 1.5 mg/kg, and 1.75 mg/kg respectively. The starting dose was chosen as a dose intermediate between the dose used to treat osteoporosis (approximately 0.9 mg/kg every six months) and the dose used to treat giant cell tumor of bone (1.7 mg/kg once monthly).

After seven months of treatment the patient fell out of bed at home and fractured his femur. The fracture occurred at the distal end of an intramedullary rod, which served as a stress riser and a predisposing site for fracture (Fig 3A). Due to a theoretical risk of delayed fracture healing, the eighth dose of denosumab was held. Shortly thereafter the patient's family lost contact with the research team.

Endpoints

The primary endpoint of denosumab efficacy was the rate of change in tumor volume as measured by CT. Additional efficacy endpoints were bone turnover markers (BTMs) and pain. Safety endpoints were signs and symptoms of infection, effects on dentition, and linear growth. Endpoints were assessed as indicated in Fig. 2.

Lesion volume was assessed by a semi-automatic approach using a Vitrea® workstation (Vital Images Inc., MN). An operator first placed a seed point inside the center of the lesion. The computer program then learned the intensity and texture pattern in the vicinity of the seed point and expanded the region in three-dimension (3D) to include pixels with similar intensity and texture as that within the lesion. The lesion region was then smoothed to close gaps and form a solid 3D object. The volume of the lesion was obtained by counting the pixels inside the 3D object.

BTMs were measured for the formation marker procollagen type 1 amino-terminal propeptide (P1NP, Radioimmunoassay, Mayo Medical Laboratories) and the resorption marker beta crosslaps of type I collagen c-telopeptide-related fraction (B-CTX, Electrochemiluminescence Immunoassay, Mayo Medical Laboratories). Arm span was measured as a surrogate for linear growth. Dental examinations, which included dental panographic and selected periapical radiographs to determine dental development and morphology were performed at baseline and after three months of treatment.

RANKL immunohistochemistry was performed on paraffin embedded sections. Sections were deparaffinized and then antigen retrieval was performed using a heat induced sodium citrate buffer method. Primary antibody reaction was performed using a monoclonal anti-RANKL antibody (Novus Biologicals, Littleton, CO; NB 100-56512) at 1 to 200 dilution incubated overnight at 4 C. Sections were then washed and incubated successfully with the biotinylated secondary antibody (Vector Laboratories, Burlingame, CA; BA-9200) at 1 to 400 dilution for 30 minutes at room temperature. VECTASTAIN ABC method (Vector Laboratories, Burlingame, CA; PK-4000) was used and the slides were then developed under direct microscopic visualization using Sigma-Aldrich SIGMAFAST™ 3, 3'-diaminobenzidine (Sigma-Aldrich Corp., St. Louis, MO; D4168).

$G_s\alpha$ mutation testing was performed on BMSCs obtained from a bone biopsy prior to treatment with denosumab. Single colonies of cells were grown separately and total DNA was isolated using Wizard genomic DNA isolation kit (Promega, WI). DNA from multiple colonies was PCR amplified and sequenced for subsequent $G_s\alpha$ genotyping. Total DNA was isolated from individual BMSC colonies and used for amplification reactions to enrich for the $G_s\alpha$-specific genomic regions by using two specific oligonucleotides: 5'-TGACTATGTGCCGAGCGATC-3' and 5'-CCACGTCAAACATGCTGGTG-3'. PCR products were gel purified and were subsequently sequenced.

RESULTS

Tumor volume

Tumor volume was assessed at four time points: 13.5 months prior to initiation of denosumab, at the initiation of denosumab treatment, and after three and nine months of treatment. The volume of FD in the left femur increased 57% between the initial scan and the scan done at the start of denosumab (Fig 4). Assuming a linear rate of expansion over this 13.5 month period, tumor volume increased at a rate of 4.2% per month. However, per report of the patient's mother and orthopedic surgeon, the expansion began acutely and progressed rapidly over a six week period immediately preceding the initiation of denosumab. Assuming the tumor growth occurred during this 1.5 month period, tumor volume increased at a rate of 37.7% per month (Fig. 4C dashed line). The rate of tumor growth was additionally calculated after three and nine months of treatment. During these intervals the rate of growth was 1.4% per month and 0.56% per month, respectively (Fig. 4C).

Additional endpoints

BTMs were significantly elevated at baseline, declined dramatically after the first dose of denosumab, and remained suppressed throughout the duration of treatment (Fig 5A&B). Narcotic-requiring pain diminished dramatically after initiation of denosumab. After one dose the patient was able to discontinue narcotics in favor of ibuprofen, and after three doses was able to stop analgesics altogether (Fig 2). A dental exam was done at baseline and three months after the start of denosumab treatment. At baseline, healthy and normal dentition with mild dental developmental delay was noted, and at follow-up, no deleterious effects were seen. Hand radiographs were monitored every three months to assess for tubulation defects and deleterious effects on the growth plate. The shapes of the bones were preserved, and there were no obvious signs of rickets, however the patient developed thick sclerotic bands at the level of the metaphyses (Fig. 3 C-F).

A bone biopsy was obtained prior to treatment start (Fig 6A), and revealed sections of typical fibrous tissue and woven bone, but also striking abundance of cartilage that accounted for most of the tissue in many sections. Osteoclasts were rare.

Immunohistochemical staining was markedly positive for RANKL (Fig. 6B). Sequencing of DNA extracted from biopsy tissue and PCR amplified revealed a typical mutation in exon 8 of *GNAS* that resulted in substitution of histidine for arginine at amino acid position 201 (R201H) (Fig. 7).

The patient became hypophosphatemic with secondary hyperparathyroidism shortly after receiving the first dose of denosumab, necessitating supplementation with phosphorus, calcitriol and calcium. Blood phosphorus and calcium levels are shown in Figure 5C&D.

The patient underwent plate fixation of the left femur, and a second biopsy specimen was obtained. The orthopedic surgeon (FAF) reported the quality of the bone appeared to be subjectively improved as compared to pre-denosumab treatment. Samples were taken at the time of the surgery, but the specimens were taken from areas of cortical bone and comparison to pre-treatment sections was not informative. Radiographs taken four weeks after fixation showed callus formation at the fracture site (Fig 3B), and plans were being made to resume denosumab, but due to unforeseen social issues the patient was temporarily lost to follow-up.

Response to cessation of denosumab

Two months after the fracture and cessation of denosumab, the patient presented to his local emergency department with five days of vomiting. Labs revealed severe hypercalcemia with a level of 4.5 mmol/L (18 mg/dL) (normal 2.1-2.6). Phosphorus and creatinine were normal, and PTH, PTHrP, and 1,25-vitamin D were suppressed. Bone turnover markers were extremely elevated. B-CTX had returned to approximately baseline levels, but P1NP had rebounded to a level approximately 2.5 fold above the pretreatment level (Fig 5C & D).

The patient was admitted to the hospital and treated with IV hydration, calcitonin and pamidronate. Calcium levels improved, but he remained mildly hypercalcemic as an outpatient, necessitating repeated treatment with intravenous bisphosphonates (pamidronate or zoledronic acid). BTMs gradually returned to baseline after approximately five months (146 days) following denosumab discontinuation, after which the hypercalcemia resolved.

DISCUSSION

In this child with a rapidly expanding FD lesion, treatment with denosumab was associated with a marked decrease in the rate of tumor growth. Expansion of FD at this rate is a rare but potentially devastating complication. Currently no medical therapies are capable of altering the disease course of FD, which makes this child's response to RANKL inhibition of particular interest. The mechanism by which this effect occurred is not clear. The accepted mechanism of action of denosumab in the treatment of osteoporosis is inhibition of osteoclastogenesis by disruption of stromal cell/osteoblast – osteoclast RANK – RANKL interaction. This may have been operative here, as osteoclastic resorption of normal bone adjacent to FD is likely involved in lesion expansion. In rapidly expanding lesions such as this, stromal cell proliferation is likely the more important mechanism of expansion. In osteoporosis inhibition of osteoclastogenesis is also accompanied by a concomitant and parallel inhibition of bone formation, as evidenced by the marked decrease in markers of bone formation, and marked inhibition of bone formation, as seen by histomorphometry (23,33). In denosumab treatment of giant cell granulomas, which like FD are tumors composed primarily of fibroblast-like cells of BMSC lineage, there is also inhibition of tumor growth (32). Additionally, RANKL inhibition has been shown to have direct inhibitory effects on other tumors such as breast cancer (24,25). Taken together, these data suggest that denosumab treatment of FD may have direct effects (or possibly indirect effects

mediated by an as yet unidentified osteoclast-derived factor) on the proliferating bone marrow stromal-derived cells that dominate FD lesions.

While promising, whether the response to denosumab seen in this child will be replicated in other individuals with FD remains to be seen. His presentation was atypical in both the growth pattern (rapid onset and marked expansion), and histologically. Specimens from both the amputated right leg (not shown) and the lesion monitored during treatment revealed large areas of cartilaginous tissue and a relative paucity of osteoclasts. While small cartilaginous foci are not uncommon in FD, extensive cartilaginous proliferation as seen here is a rare but previously-described phenomenon (34-36). The demonstration of a typical *GNAS* mutation in this lesion, the first time this has been demonstrated in this variant of FD, confirms that this molecular defect is at least partially responsible for the phenotype. However, the prominence of cartilage seen in this specimen clearly marks the FD in this patient as atypical. Whether or not denosumab will have similar efficacy in typical FD is not known. The fact that RANKL expression is prominent in a model of FD (17) and that RANKL expression, as seen by immunohistochemistry, can be seen in more histologically typical FD lesions (personal observations, MTC), is encouraging that it may.

The pretreatment rate of growth in this child was an estimate based upon a combination of imaging data and observations of the patient's mother and orthopedist. This resulted in a degree of uncertainty in determining the exact rate of growth and the precise effect of denosumab treatment on the rate of growth. While it is possible that the lesion had undergone a significant but time-limited period of expansion, and that the initiation of denosumab was coincidental, this is probably less likely than the possibility that denosumab had a direct effect on lesion expansion. An effect by denosumab is supported by what occurred in the right femur, i.e. rapid and progressive expansion until amputation. Additional studies are needed to assess potential efficacy in FD.

Important and potentially serious side effects occurred as a result of treatment with denosumab: secondary hyperparathyroidism and hypophosphatemia during denosumab treatment, and severe hypercalcemia on discontinuation. The likely cause of secondary hyperparathyroidism was combined inhibition of osteoclast mediated calcium release from bone and FGF23-mediated suppression of 1,25 $(OH)_2$-vitamin D generation. As is seen in extensive FD, serum FGF23 was elevated at 95.5 pg/mL (normal 20-50), but FGF23 levels did not change significantly throughout treatment. However, upon discontinuation of denosumab there was a marked rebound in BTMs (CTX rose to 2.5-fold greater than the pre-treatment levels), with a proportionally greater rebound in the resorption marker CTX than the formation marker P1NP. BTM levels peaked at approximately 90 days after denosumab discontinuation, and returned to pre-treatment levels after 146 days (approximately 5 months). While a similar pattern of changes in BTMs has been seen in patients with osteoporosis (37), there are important differences. Relative to patients with osteoporosis, there was a similar marked and pronounced decline in both resorption and formation markers. However upon discontinuation the rebound was more rapid in this patient (3 mo. vs. 6 mo.), the rebound to levels above baseline was confined to the resorption marker, the level of resorption marker rebound was much greater, (250% vs. 60%), and the return to baseline was much shorter (5 mo. vs. 24 mo.). Of note, the rapidity of return to baseline in this child was enhanced by treatment with bisphosphonates. Hypercalcemia has not been previously reported in association with denosumab discontinuation in osteoporosis studies where follow-up has been continued for relatively long periods. While hypercalcemia after denosumab discontinuation has not been reported in cancer studies, where the doses are higher, adverse event monitoring is not as long as the follow-up in osteoporosis studies. The marked rebound seen in this patient may be due to some combination of very active FD and a higher rate of bone metabolism in a growing

child. Due to the severity of the associated adverse effects, practitioners should be cautious in using denosumab in patients with FD, and should consider limiting use to clinical trials and in individuals with extremely severe disease.

Preclinical studies with denosumab in rodents and primates demonstrated a significant inhibitory effect on linear growth and tooth eruption (38,39). In our patient there was no increase in arm span over a six month period, which may represent impaired linear growth as a complication of treatment. However, six months is possibly too short of a period of time for determination of growth velocity, and measurement of arm span in this patient was technically difficult due to pain and impaired mobility. The increase in primary spongiosa at the level of the epiphyses that was observed as an area of sclerosis on the radiographs suggests that growth was occurring. Nonetheless growth impairment should be monitored as a potential adverse effect of denosumab in children. Hand and knee X-rays showed no clear impairment in bone tubulation or geometry during the treatment period, however thick sclerotic bands developed at the level of the metaphyses, consistent with profound suppression in bone turnover. These findings are similar to those seen in children treated with bisphosphonates (40,41), and represent accumulation of calcified cartilage from bisphosphonate-induced inhibition of peri-epiphyseal cartilage resorption.

While the femoral fracture that occurred while on treatment was traumatic in nature, a contributory role of denosumab treatment cannot be excluded. Atypical femur fractures have been reported with antiresorptive treatment (42), however this typically only occurs after years of treatment. In addition, fractures are a known complication of FD, and this patient had sustained two previous FD-related femoral fractures prior to treatment with denosumab. Consistent with what has been seen in preclinical studies with denosumab, there was no apparent disruption of fracture healing (43).

CONCLUSIONS

In this child with FD, denosumab was effective for both prevention of lesion expansion and FD-related bone pain. Denosumab treatment was associated with predictable, clinically significant side effects both during treatment (hypophosphatemia and secondary hyperparathyroidism) and on discontinuation (hypercalcemia) that necessitated careful monitoring and additional medications both during treatment and upon discontinuation. Denosumab treatment of FD warrants further study, not only to confirm efficacy and determine potential morbidity, but also to study the mechanism of RANKL in the pathogenesis of FD and related BMSC diseases.

Acknowledgments

This research was supported by the Intramural Research Program of the NIH, NIDCR.

Authors' roles: Study design: AMB, RIG, and MTC. Study conduct: AMB, RIG, MHK, CEC, ME, JZK, and MTC. Data collection: AMB, WHC, JY, MHK, CEC, CB, NC, ME, JZK, FAF, NB and MTC. Data analysis: AMB, WHC, JY, CB, NC, FAF, AAM, NB, and MTC. Data interpretation: AMB, WHC, CB, NC, FAF, AAM, NB, and MTC. Drafting manuscript: AMB, WHC, JY, CB, NB, and MTC. Revising manuscript content: AMB, WHC, JY, RIG, MHK, CEC, CB, NC, ME, JZK, FAF, AAM, NB, and MTC. Approving final version of manuscript: AMB, WHC, JY, RIG, MHK, CEC, CB, NC, ME, JZK, FAF, AAM, NB, and MTC. AMB and MTC take responsibility for the integrity of the data analysis.

REFERENCES

1. Collins, MT.; Bianco, P. Fibrous dysplasia.. In: Favus, MJ., editor. Primer on the Metabolic Bone Diseases and Disorders of Mineral Metabolism. 6ed.. American Society for Bone and Mineral Research; Washington, D.C.: 2006. p. 415-418.

2. Lichtenstein L. Poloyostotic fibrous dysplasia. Arch Surg. 1938; 36:874–898.
3. Lichtenstein L, Jaffe HL. Fibrous dysplasia of bone: a condition affecting one, several or many bones, the graver cases of which may present abnormal pigmentation of skin, premature sexual development, hyperthyroidism or still other extraskeletal abnormalities. ArchPathol. 1942; 33:777–816.
4. McCune DJ. Osteitis fibrosa cystica; the case of a nine year old girl who also exhibits precocious puberty, multiple pigmentation of the skin and hyperthyroidism. Am J Dis Child. 1936; 52:743–744.
5. Albright F, Butler AM, Hampton AO, Smith PH. Syndrome characterized by osteitis fibrosa disseminata, areas of pigmentation and endocrine dysfunction, with precocious puberty in females, report of five cases. N Engl J Med. 1937; 216:727–746.
6. Dumitrescu CE, Collins MT. McCune-Albright syndrome. Orphanet journal of rare diseases. 2008; 3:12. [PubMed: 18489744]
7. Collins MT, Chebli C, Jones J, Kushner H, Consugar M, Rinaldo P, Wientroub S, Bianco P, Robey PG. Renal phosphate wasting in fibrous dysplasia of bone is part of a generalized renal tubular dysfunction similar to that seen in tumor-induced osteomalacia. J Bone Miner Res. 2001; 16(5): 806–813. [PubMed: 11341325]
8. Riminucci M, Collins MT, Fedarko NS, Cherman N, Corsi A, White KE, Waguespack S, Gupta A, Hannon T, Econs MJ, Bianco P, Gehron Robey P. FGF-23 in fibrous dysplasia of bone and its relationship to renal phosphate wasting. J Clin Invest. 2003; 112(5):683–692. [PubMed: 12952917]
9. Weinstein LS, Shenker A, Gejman PV, Merino MJ, Friedman E, Spiegel AM. Activating mutations of the stimulatory G protein in the McCune-Albright syndrome. N Engl J Med. 1991; 325(24): 1688–1695. [PubMed: 1944469]
10. Schwindinger WF, Francomano CA, Levine MA. Identification of a mutation in the gene encoding the α subunit of the stimulatory G protein of adenylyl cyclase in McCune-Albright syndrome. Proc Natl Acad Sci USA. 1992; 89:5152–5156. [PubMed: 1594625]
11. Happle R. The McCune-Albright syndrome: a lethal gene surviving by mosaicism. Clin Genet. 1986; 29:321–324. [PubMed: 3720010]
12. Riminucci M, Saggio I, Robey PG, Bianco P. Fibrous dysplasia as a stem cell disease. J Bone Miner Res 21 Suppl. 2006; 2:P125–131.
13. Riminucci M, Gehron Robey P, Saggio I, Bianco P. Skeletal progenitors and the GNAS gene: fibrous dysplasia of bone read through stem cells. Journal of molecular endocrinology. 2010
14. Riminucci M, Fisher LW, Shenker A, Spiegel AM, Bianco P, Gehron Robey P. Fibrous dysplasia of bone in the McCune-Albright syndrome: abnormalities in bone formation. The American journal of pathology. 1997; 151(6):1587–1600. [PubMed: 9403710]
15. Riminucci M, Liu B, Corsi A, Shenker A, Spiegel AM, Robey PG, Bianco P. The histopathology of fibrous dysplasia of bone in patients with activating mutations of the Gs alpha gene: site-specific patterns and recurrent histological hallmarks. J Pathol. 1999; 187(2):249–258. [PubMed: 10365102]
16. Bianco P, Kuznetsov SA, Riminucci M, Fisher LW, Spiegel AM, Robey PG. Reproduction of human fibrous dysplasia of bone in immunocompromised mice by transplanted mosaics of normal and Gsalpha-mutated skeletal progenitor cells. J Clin Invest. 1998; 101(8):1737–1744. [PubMed: 9541505]
17. Piersanti S, Remoli C, Saggio I, Funari A, Michienzi S, Sacchetti B, Robey PG, Riminucci M, Bianco P. Transfer, analysis, and reversion of the fibrous dysplasia cellular phenotype in human skeletal progenitors. J Bone Miner Res. 2010; 25(5):1103–1116. [PubMed: 19874199]
18. Stanton RP. Surgery for fibrous dysplasia. J Bone Miner Res. 2006; 21(Suppl 2):P105–109. [PubMed: 17228997]
19. Collins MT, Kushner H, Reynolds JC, Chebli C, Kelly MH, Gupta A, Brillante B, Leet AI, Riminucci M, Robey PG, Bianco P, Wientroub S, Chen CC. An instrument to measure skeletal burden and predict functional outcome in fibrous dysplasia of bone. J Bone Miner Res. 2005; 20(2):219–226. [PubMed: 15647815]
20. Parisi MS, Oliveri B, Mautalen CA. Effect of intravenous pamidronate on bone markers and local bone mineral density in fibrous dysplasia. Bone. 2003; 33(4):582–588. [PubMed: 14555262]

21. Plotkin H, Rauch F, Zeitlin L, Munns C, Travers R, Glorieux FH. Effect of pamidronate treatment in children with polyostotic fibrous dysplasia of bone. J Clin Endocrinol Metab. 2003; 88(10): 4569–4575. [PubMed: 14557424]
22. Fizazi K, Bosserman L, Gao G, Skacel T, Markus R. Denosumab treatment of prostate cancer with bone metastases and increased urine N-telopeptide levels after therapy with intravenous bisphosphonates: results of a randomized phase II trial. The Journal of urology. 2009; 182(2):509–515. discussion 515-506. [PubMed: 19524963]
23. McClung MR, Lewiecki EM, Cohen SB, Bolognese MA, Woodson GC, Moffett AH, Peacock M, Miller PD, Lederman SN, Chesnut CH, Lain D, Kivitz AJ, Holloway DL, Zhang C, Peterson MC, Bekker PJ. Denosumab in postmenopausal women with low bone mineral density. N Engl J Med. 2006; 354(8):821–831. [PubMed: 16495394]
24. Gonzalez-Suarez E, Jacob AP, Jones J, Miller R, Roudier-Meyer MP, Erwert R, Pinkas J, Branstetter D, Dougall WC. RANK ligand mediates progestin-induced mammary epithelial proliferation and carcinogenesis. Nature. 2010; 468(7320):103–107. [PubMed: 20881963]
25. Schramek D, Leibbrandt A, Sigl V, Kenner L, Pospisilik JA, Lee HJ, Hanada R, Joshi PA, Aliprantis A, Glimcher L, Pasparakis M, Khokha R, Ormandy CJ, Widschwendter M, Schett G, Penninger JM. Osteoclast differentiation factor RANKL controls development of progestin-driven mammary cancer. Nature. 2010; 468(7320):98–102. [PubMed: 20881962]
26. Mikami S, Katsube K, Oya M, Ishida M, Kosaka T, Mizuno R, Mochizuki S, Ikeda T, Mukai M, Okada Y. Increased RANKL expression is related to tumour migration and metastasis of renal cell carcinomas. The Journal of pathology. 2009; 218(4):530–539. [PubMed: 19455604]
27. Sasaki A, Ishikawa K, Haraguchi N, Inoue H, Ishio T, Shibata K, Ohta M, Kitano S, Mori M. Receptor activator of nuclear factor-kappaB ligand (RANKL) expression in hepatocellular carcinoma with bone metastasis. Annals of surgical oncology. 2007; 14(3):1191–1199. [PubMed: 17195907]
28. Roodman GD, Dougall WC. RANK ligand as a therapeutic target for bone metastases and multiple myeloma. Cancer treatment reviews. 2008; 34(1):92–101. [PubMed: 17964729]
29. Stopeck AT, Lipton A, Body JJ, Steger GG, Tonkin K, de Boer RH, Lichinitser M, Fujiwara Y, Yardley DA, Viniegra M, Fan M, Jiang Q, Dansey R, Jun S, Braun A. Denosumab compared with zoledronic acid for the treatment of bone metastases in patients with advanced breast cancer: a randomized, double-blind study. Journal of clinical oncology : official journal of the American Society of Clinical Oncology. 2010; 28(35):5132–5139. [PubMed: 21060033]
30. Fizazi K, Carducci M, Smith M, Damiao R, Brown J, Karsh L, Milecki P, Shore N, Rader M, Wang H, Jiang Q, Tadros S, Dansey R, Goessl C. Denosumab versus zoledronic acid for treatment of bone metastases in men with castration-resistant prostate cancer: a randomised, double-blind study. Lancet. 2011; 377(9768):813–822. [PubMed: 21353695]
31. Molyneux SD, Di Grappa MA, Beristain AG, McKee TD, Wai DH, Paderova J, Kashyap M, Hu P, Maiuri T, Narala SR, Stambolic V, Squire J, Penninger J, Sanchez O, Triche TJ, Wood GA, Kirschner LS, Khokha R. Prkar1a is an osteosarcoma tumor suppressor that defines a molecular subclass in mice. J Clin Invest. 2010; 120(9):3310–3325. [PubMed: 20697156]
32. Thomas D, Henshaw R, Skubitz K, Chawla S, Staddon A, Blay JY, Roudier M, Smith J, Ye Z, Sohn W, Dansey R, Jun S. Denosumab in patients with giant-cell tumour of bone: an open-label, phase 2 study. The lancet oncology. 2010; 11(3):275–280. [PubMed: 20149736]
33. Reid IR, Miller PD, Brown JP, Kendler DL, Fahrleitner-Pammer A, Valter I, Maasalu K, Bolognese MA, Woodson G, Bone H, Ding B, Wagman RB, San Martin J, Ominsky MS, Dempster DW. Effects of denosumab on bone histomorphometry: the FREEDOM and STAND studies. J Bone Miner Res. 2010; 25(10):2256–2265. [PubMed: 20533525]
34. Pelzmann KS, Nagel DZ, Salyer WR. Case report 114. Skeletal radiology. 1980; 5(2):116–118. [PubMed: 7375958]
35. Ishida T, Dorfman HD. Massive chondroid differentiation in fibrous dysplasia of bone (fibrocartilaginous dysplasia). The American journal of surgical pathology. 1993; 17(9):924–930. [PubMed: 8352377]
36. Kyriakos M, McDonald DJ, Sundaram M. Fibrous dysplasia with cartilaginous differentiation ("fibrocartilaginous dysplasia"): a review, with an illustrative case followed for 18 years. Skeletal radiology. 2004; 33(1):51–62. [PubMed: 14647989]

37. Bone HG, Bolognese MA, Yuen CK, Kendler DL, Miller PD, Yang YC, Grazette L, San Martin J, Gallagher JC. Effects of denosumab treatment and discontinuation on bone mineral density and bone turnover markers in postmenopausal women with low bone mass. J Clin Endocrinol Metab. 2011; 96(4):972–980. [PubMed: 21289258]

38. Kong YY, Yoshida H, Sarosi I, Tan HL, Timms E, Capparelli C, Morony S, Oliveira-dos-Santos AJ, Van G, Itie A, Khoo W, Wakeham A, Dunstan CR, Lacey DL, Mak TW, Boyle WJ, Penninger JM. OPGL is a key regulator of osteoclastogenesis, lymphocyte development and lymph-node organogenesis. Nature. 1999; 397(6717):315–323. [PubMed: 9950424]

39. Package Insert P.

40. van Persijn van Meerten EL, Kroon HM, Papapoulos SE. Epi- and metaphyseal changes in children caused by administration of bisphosphonates. Radiology. 1992; 184(1):249–254. [PubMed: 1609087]

41. Rauch F, Travers R, Munns C, Glorieux FH. Sclerotic metaphyseal lines in a child treated with pamidronate: histomorphometric analysis. Journal of bone and mineral research : the official journal of the American Society for Bone and Mineral Research. 2004; 19(7):1191–1193. [PubMed: 15177003]

42. Giusti A, Hamdy NA, Papapoulos SE. Atypical fractures of the femur and bisphosphonate therapy: A systematic review of case/case series studies. Bone. 2010; 47(2):169–180. [PubMed: 20493982]

43. Gerstenfeld LC, Sacks DJ, Pelis M, Mason ZD, Graves DT, Barrero M, Ominsky MS, Kostenuik PJ, Morgan EF, Einhorn TA. Comparison of effects of the bisphosphonate alendronate versus the RANKL inhibitor denosumab on murine fracture healing. J Bone Miner Res. 2009; 24(2):196–208. [PubMed: 19016594]

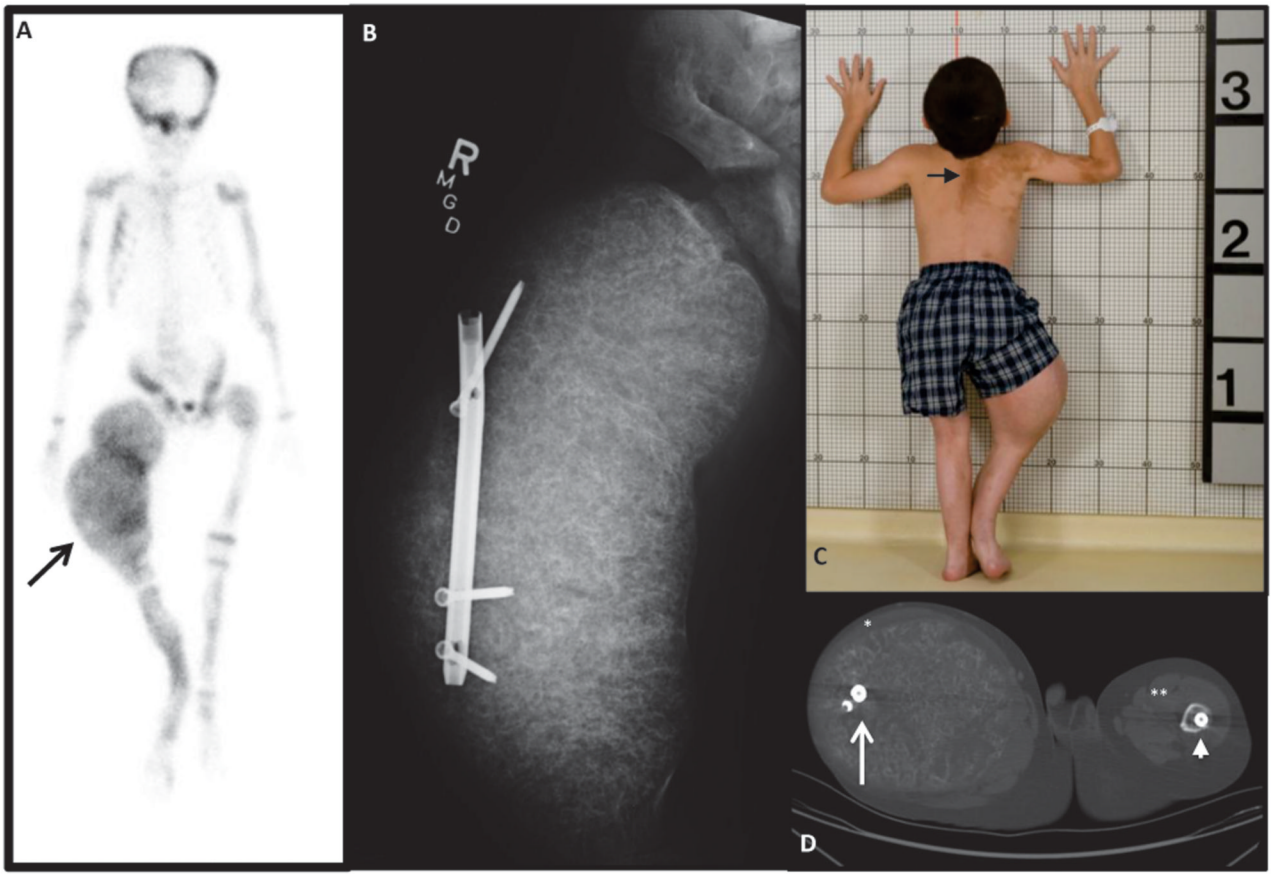

Figure 1. Initial Clinical Presentation

A) ^{99}Technectium-MDP bone scan showing extensive tracer uptake at multiple areas of FD and ballooning expansion of the right femur (arrow). B) X-ray shows massive expansion of right femur and displacement of a rod that was originally in the intramedullary canal. C) Photograph showing classic “coast-of-Maine” café-au-lait spots (arrow) and the effect of massive overgrowth of the right femur. D) CT at the level of the femura mid-shafts, with lateral displacement of the rod on the right (white arrow), and an intramedullary rod on the left (arrow head). The quadriceps muscles on the right have been stretched to dysfunctional bands (*), compared to the left (**).

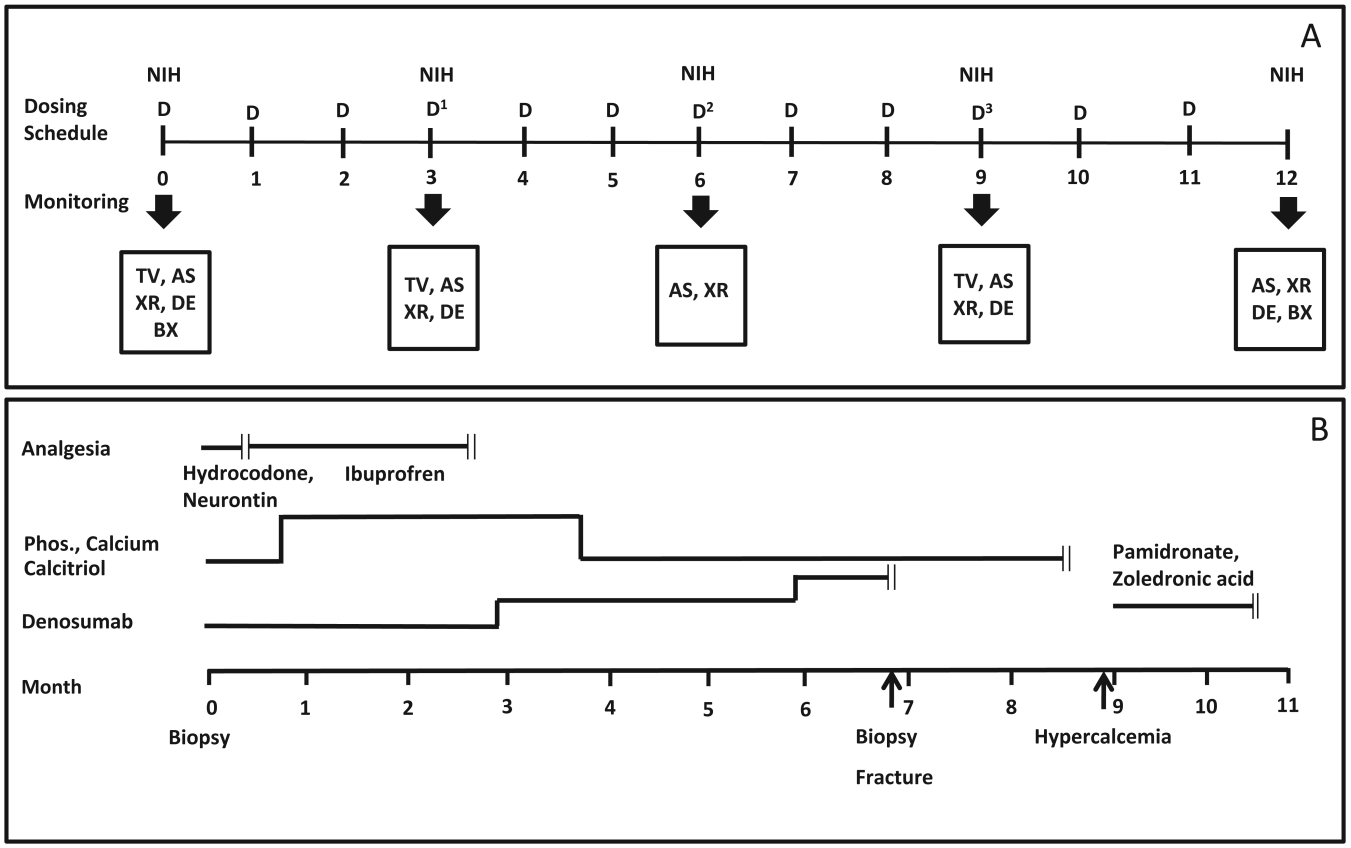

Figure 2. Proposed treatment regimen and clinical course

A) Proposed Regimen. Dosing regimen and monitoring schedule are indicated. Denosumab was to be given monthly at an initial dose of 1 mg/kg. Dose escalations were planned at three month intervals (blue arrows) to 1.25 mg/kg, 1.5 mg/kg, and 1.75 mg/kg. The patient was evaluated by his local endocrinologist monthly and at NIH every three months. Mineral panels were monitored weekly for the first three months and then monthly (not shown). Bone turnover markers were monitored monthly (not shown). The scale represents months. D = dose of denosumab, TV = tumor volume, AS = arm spam, XR = Hand XR, DE = dental exam, BX = bone biopsy. B) Clinical Course. The periods for the administration of analgesics, supplemental phosphorus, calcium and calcitriol, denosumab, and bisphosphonate treatment (pamidronate or zoledronic acid) are indicated by the transverse lines, and cessation by the double vertical lines. Time points for biopsy, fracture and start of hypercalcemia are indicated. The scale represents months.

Figure 3. Radiographs

A) A radiograph at the time of fracture indicated the fracture occurred at the distal end of a previously intramedullary rod (longer arrow). B. Eight weeks after lplate fixation shows callus formation at the fracture site (arrow). C&D) Knee radiographs pre-treatment and 6 months after the initiation of treatment, as indicated. E&F) Hand radiographs, as above. Note the thick sclerotic bands at the level of the metaphyses (arrows), reminiscent of the radiologic appearance of children treated with bisphosphonates. There does not appear to be evidence of frank rickets.

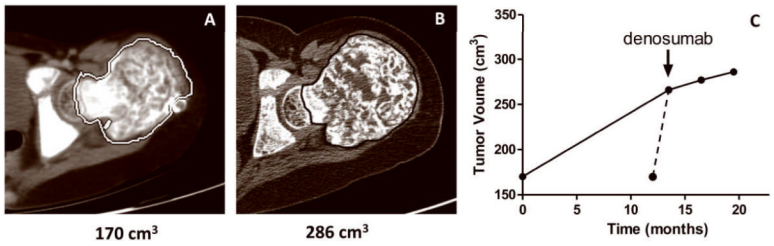

Figure 4. Tumor volume

A) A representative two dimensional image created from a horizontal slice prior to denosumab treatment at the level of the femoral head taken from a thin slice CT study that was used to measure tumor volume (see Methods). B) A similar image taken two months after the final dose of denosumab. C) This panel shows the change in tumor volume over time. The first and last time points were derived from the studies done for panels A&B. The start of denosumab treatment is indicated. There were 13.5 months between the initial study and the scan done prior to start of denosumab. The solid line represents the change in volume assuming a linear rate of growth. Per report of the patient's mother and orthopedic surgeon, expansion began acutely and progressed rapidly over six weeks prior to initiation of denosumab, represented by the dashed line. Initiation of treatment was associated with marked decrease in the rate of tumor growth.

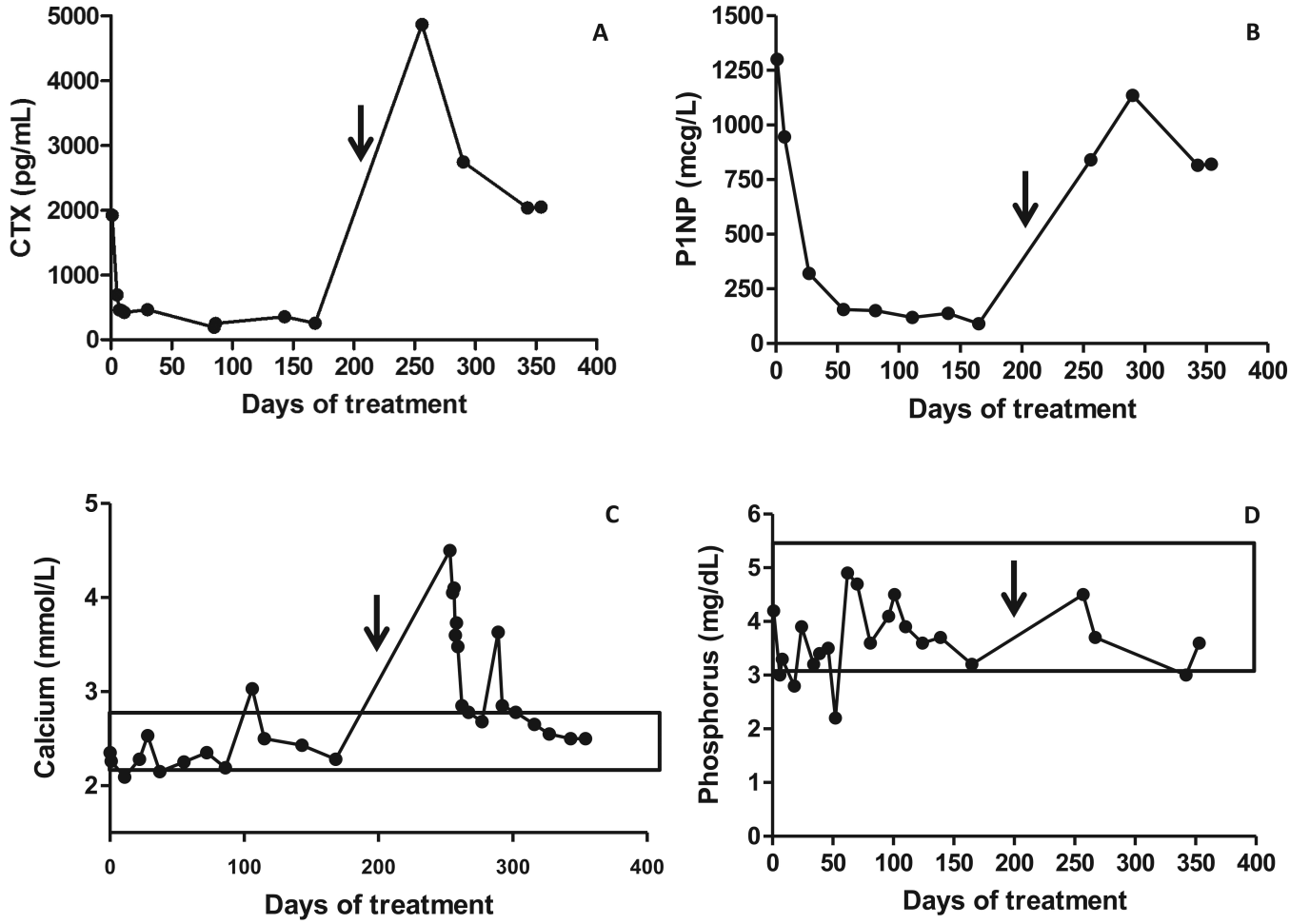

Figure 5. Biochemical Response to Treatment

A) Serum B-CTX, a marker of bone resorption. B) Serum P1NP, a marker of bone formation. C) Serum calcium. D) Serum phosphorus. Denosumab was initiated at Day 0 and discontinued at day 210, indicated by the arrow. After discontinuation of denosumab there was a marked increase in BTMs, especially the resorption marker CTX that was associated with marked hypercalcemia in the presence of a suppressed serum PTH, and 1,25 (OH)2 vitamin D. Normal ranges for calcium and phosphorus are indicated by boxes. Normal ranges for CTX and P1NP in children are not well defined.

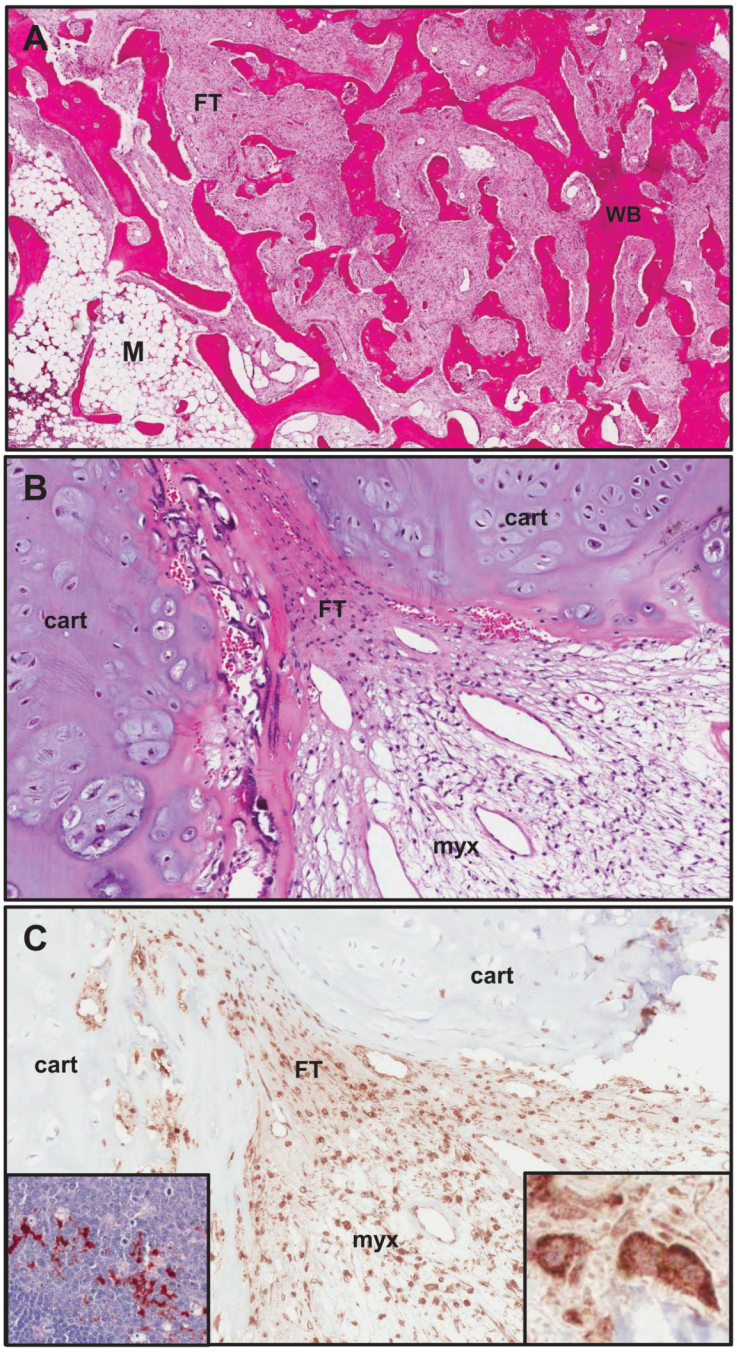

Figure 6. Histopathology

A) An H&E stained section of FD taken prior to the initiation of denosumab from a region of the lesion that demonstrated typical features of FD. The overall "Chinese character" appearance is evident and consists of areas of typical fibrous tissue (FT) interspersed amongst trabecular structures composed of woven bone (WB), as well as small region of relatively fatty bone marrow (M). B) This H&E section was from a region of the lesion that had a prominent cartilaginous component (cart), as well as areas of FT composed of stromal cells and an area with a myxoid appearance (myx), which again is sometimes seen in FD, but is not typical. C) A serial section adjacent to the area shown in panel B stained for RANKL demonstrated that most of the stromal cells were positive for RANKL with a cell

surface staining pattern, and that the chondroid cells were negative. The inset panel on the right shows a high power view of RANKL positive stromal cells and the inset panel on the left from a normal human lymph node with RANKL positive lymphoid cells served as a positive control for RANKL staining.

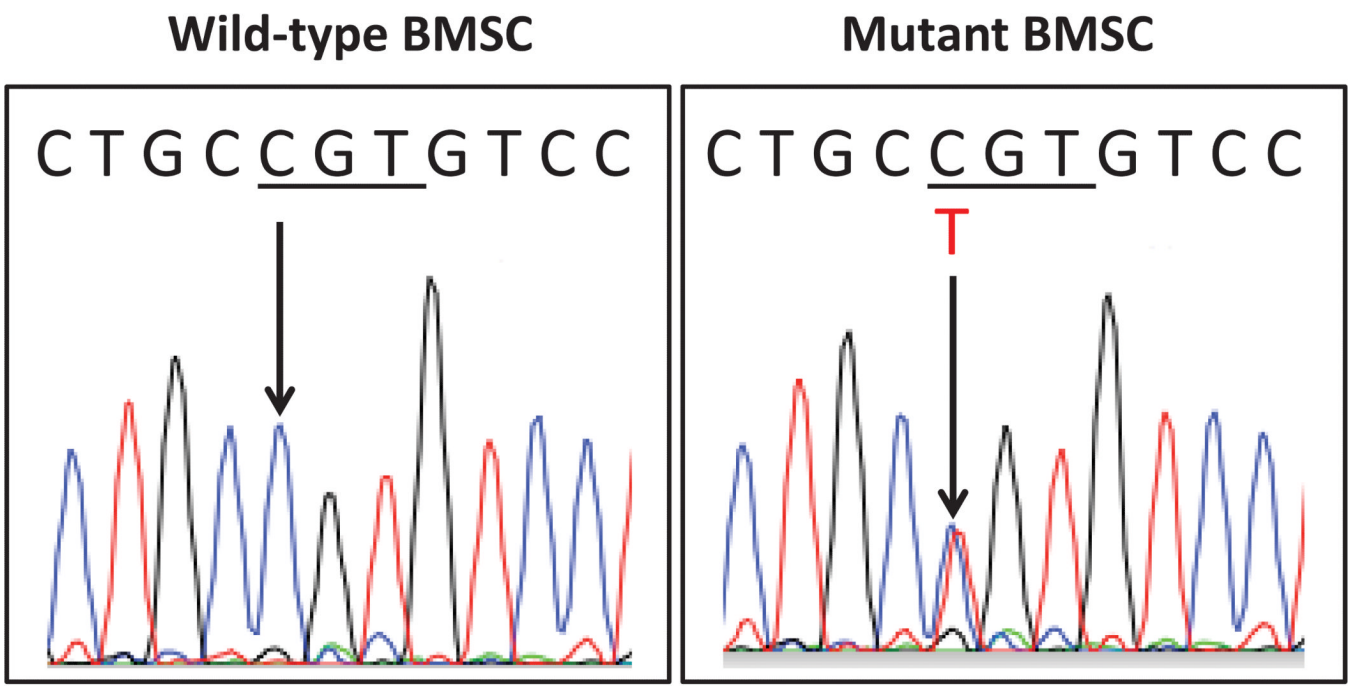

Figure 7. Mutation Analysis

BMSCs were isolated from a pre-treatment bone biopsy and expanded in vitro, as described in the Methods section. Total DNA was isolated and the mutated $G_s\alpha$-specific region was amplified. PCR products were sequenced, and DNA sequencing from the Arginine-201 region is shown. Clonal strains carrying the wild-type $G_s\alpha$ (C G T) or the heterozygous R201C mutation (C/T G T) are indicated by arrows.